Beyond the classical thermodynamic contributions to hydrogen atom abstraction reactivity

Daniel Bím[a,b], Mauricio Maldonado-Domínguez[a], Lubomír Rulíšek[b], and Martin Srnec[a,1]

[a]J. Heyrovský Institute of Physical Chemistry, Czech Academy of Sciences, Prague 8, 18223, Czech Republic; and [b]Institute of Organic Chemistry and Biochemistry, Czech Academy of Sciences, Prague 6, 16000, Czech Republic

Edited by Edward I. Solomon, Stanford University, Stanford, CA, and approved August 28, 2018 (received for review April 13, 2018)

Hydrogen atom abstraction (HAA) reactions are cornerstones of chemistry. Various (metallo)enzymes performing the HAA catalysis evolved in nature and inspired the rational development of multiple synthetic catalysts. Still, the factors determining their catalytic efficiency are not fully understood. Herein, we define the simple thermodynamic factor η by employing two thermodynamic cycles: one for an oxidant (catalyst), along with its reduced, protonated, and hydrogenated form; and one for the substrate, along with its oxidized, deprotonated, and dehydrogenated form. It is demonstrated that η reflects the propensity of the substrate and catalyst for (a)synchronicity in concerted H^+/e^- transfers. As such, it significantly contributes to the activation energies of the HAA reactions, in addition to a classical thermodynamic (Bell–Evans–Polanyi) effect. In an attempt to understand the physicochemical interpretation of η, we discovered an elegant link between η and reorganization energy λ from Marcus theory. We discovered computationally that for a homologous set of HAA reactions, λ reaches its maximum for the lowest $|\eta|$, which then corresponds to the most synchronous HAA mechanism. This immediately implies that among HAA processes with the same reaction free energy, ΔG_0, the highest barrier ($\equiv\Delta G^{\neq}$) is expected for the most synchronous proton-coupled electron (i.e., hydrogen) transfer. As proof of concept, redox and acidobasic properties of nonheme $Fe^{IV}O$ complexes are correlated with activation free energies for HAA from C–H and O–H bonds. We believe that the reported findings may represent a powerful concept in designing new HAA catalysts.

reduction potential | acidity constant | reorganization energy | asynchronicity factor | hydrogen atom transfer

Hydrogen atom abstraction (HAA) is a seemingly simple process, in which an electron and proton pair is concomitantly transferred from a substrate to an oxidant (or to an oxidant/base pair) (1). One example is C–H bond homolysis by a strong oxidant, which is the rate-determining step in many chemical transformations (2, 3) and the modus operandi of many metalloenzymes in substrate activation (4). A growing body of experimental and theoretical studies dedicated to HAA chemistry has revealed its fascinating complexity (5), which concerns, among other things, (*i*) a distinction between proton-coupled electron-transfer (PCET) and hydrogen atom transfer (HAT) mechanisms (6–10); (*ii*) tunneling contributions to reactivity, as reflected by large H/D kinetic isotope effects (KIEs) and their dependence on temperature (11–13); and lastly (*iii*) a well-recognized linear/quadratic relationship (9, 14, 15) between the free energy of activation ($\Delta G^{\neq}$) and the free energy of reaction (ΔG_0). The relationship is often surrogated by the Bell–Evans–Polanyi (BEP) principle (1, 16, 17), which, strictly speaking, correlates $\Delta G^{\neq}$ with the reaction enthalpy. According to the classical thermodynamic BEP-like effect, a more exergonic reaction yields a lower $\Delta G^{\neq}$. Typically, a change in $\Delta G^{\neq}$ is about one-half of the change in ΔG_0. This has been observed within a set of reactions in which one oxidant attacks various C–H (or O–H/N–H) bonds of the substrates. However, many systems do not behave according to the BEP-like principle, as exemplified by the work of MacMillan and coworkers (18), who performed a selective activation of a stronger C–H bond in the presence of weaker ones using the quinuclidine radical cation. Instead, they attributed the observed selectivity to "polar effects", which favor stronger C–H bond due to better polarity match with the electrophilicity of the oxidizing radical. The polar effects on HAA kinetics, which may be qualitatively (and concisely) described as the following:

$$R^{\bullet}_{\text{electro/nucleophilic}} + H^{\delta+} - Y^{\delta-} \xrightarrow{\text{slow/fast}} R-H+Y^{\bullet}$$

$$R^{\bullet}_{\text{electro/nucleophilic}} + H^{\delta-} - Y^{\delta+} \xrightarrow{\text{fast/slow}} R-H+Y^{\bullet},$$

were already recognized in the 1980s and referred to as polarity matching effect (PME) by Tedder (19) and Paul and Roberts (20), the latter of whom also introduced the polarity reversal catalysis (21) strategy as an empirical guideline for C–H activation. The PME approach has been popular in organic chemistry but lacks any quantitative prediction ability. Moreover, PME rules can be difficult to apply to a broad spectrum of PCET agents, including transition-metal systems in which donors and acceptors for electron vs. proton may reside on different sites and the distinction between electrophilic and nucleophilic oxidants can be subtle or ambiguous.

Among the most powerful transition-metal–based agents capable of HAA are complexes with the reactive ferryl ($Fe^{IV}O$)

Significance

Hydrogen atom abstraction reactivity is a key property of many important biological and synthetic compounds that depends on their proton-coupled reduction potentials. These potentials quantify the ability of species to acquire an electron and proton pair. Intuitively, a species with a higher proton-coupled reduction potential abstracts hydrogen atoms more easily, which translates into a lower reaction barrier. Beyond this classical thermodynamic effect on reactivity, we discovered a significant contribution arising from a factor reflecting propensity for (a)synchronicity in concerted H^+/e^- transfers, which stems directly from the reduction potentials and acidity constants of reactants and products. We show that the most synchronous hydrogen atom abstractions tend to pass over the highest barriers, as exemplified by computations on $Fe^{IV}O$ oxidants.

Author contributions: M.S. designed research; D.B., M.M.-D., and M.S. performed research; D.B., M.M.-D., and M.S. analyzed data; and D.B., M.M.-D., L.R., and M.S. wrote the paper.

The authors declare no conflict of interest.

This article is a PNAS Direct Submission.

[1]To whom correspondence should be addressed. Email: martin.srnec@jh-inst.cas.cz.

This article contains supporting information online at www.pnas.org/lookup/suppl/doi:10.1073/pnas.1806399115/-/DCSupplemental.

Published online September 25, 2018.

unit (22). As shown in refs. 23–25, electrochemical behavior of these species may be very sensitive to the nature of even a single ligand, which also affects their HAA reactivity. This has motivated us to exploit this type of system as a model for the theoretical study of the interplay between redox and acidobasic properties of reagents and their effects on the associated HAA barriers. We attempt to unify and extend the theory for both classical (BEP) and PME principles by introducing the so-called asynchronicity factor η. This factor directly stems from the thermodynamic redox and acidobasic properties of the oxidant and the substrate and, being related to the reorganization energy from Marcus theory, is found to be an important factor in tuning the reaction barrier for an HAA process. In our opinion, this opens new opportunities in computer-aided design of catalysts operating through HAA reactions.

Results and Discussion

Electrophilicity vs. Basicity Contributions to HAA Thermodynamic Driving Force for Tetramethylcyclam (TMC)-Supported $Fe^{IV}O$ Species. Exploiting a recently developed methodology for the accurate calculation of (proton-coupled) reduction potentials, which has been validated on a broad set of mononuclear nonheme iron complexes, including the $Fe^{IV}O$ species (26), we further probed redox and acidobasic properties of these high-valent species and correlated them with their HAA barriers (*SI Appendix, Computational Details*).

To this aim, we conceived a series of 19 (X)(TMC)$Fe^{IV}O$ model complexes that differ in the ligand X (Fig. 1). The one-electron reduction potentials of these $Fe^{IV}O$ complexes range from +0.4 to −0.8 V (at 298 K in CH_3CN using the SCE reference redox couple), which mainly depends on the electron-donating ability of the axial ligand X (Fig. 1). The ferryl complex with the least electron-donating axial ligand, CO, exhibits the highest reduction potential (+0.39 V). In contrast, the reduction potential is lowered by >1 V when CO is replaced by the strong electron donor NH_2^-. This trend in the reduction potentials ($E°$) is opposite to the trend in the acidity constants (pK_a); the lowest pK_a is found for the CO-bound ferryl complex, and it increases by around 20 pK_a units upon going to the NH_2-bound ferryl complex. Qualitatively, the strongest (X)(TMC)$Fe^{IV}O$ oxidant is the weakest base, and vice versa.

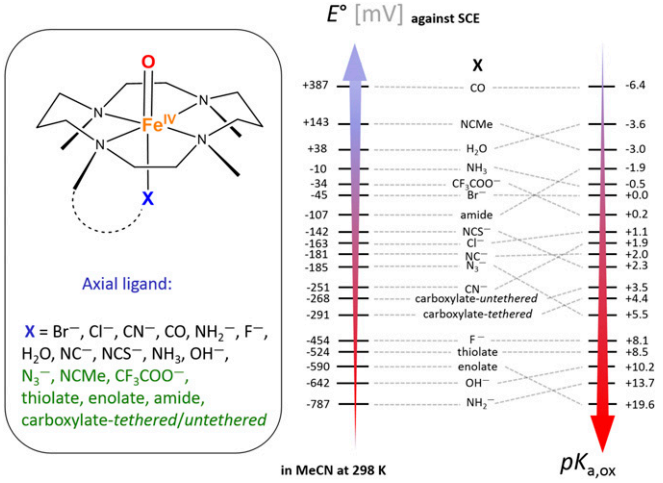

Fig. 1. (*Left*) The set of 19 $Fe^{IV}O$ complexes, all supported by the TMC ligand, that differ in the axial ligand X. The ferryl complexes, for which the X ligands are highlighted in green, were experimentally characterized in refs. 23–25. (*Right*) The calculated one-electron reduction potentials vs. acidity constants, as measures of electrophilicity vs. basicity of the (X)(TMC)$Fe^{IV}O$ complexes.

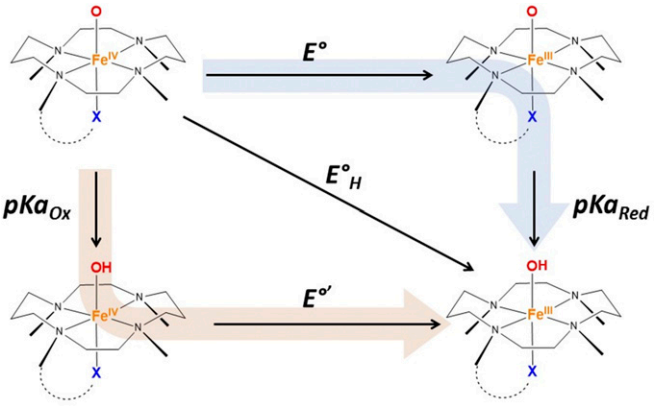

Scheme 1. The thermodynamic cycle connecting four structures that differ by one electron (horizontal arrows), one proton (vertical arrows), and a hydrogen atom (diagonal arrow), along with the associated thermodynamic quantities: $E°$ and $E°'$ – $1e^-$ reduction potential of the $Fe^{IV}O$ and its protonated form ($Fe^{IV}OH$), respectively; $pK_{a,ox}$ and $pK_{a,red}$ – acidity constant of the oxidized ($Fe^{IV}OH$) and reduced ($Fe^{III}OH$) species, respectively; and $E°_H$ – proton-coupled $1e^-$ reduction potential of $Fe^{IV}O$.

Proton-coupled reduction potential ($E°_H$), quantifying the ability of a system to abstract a hydrogen atom, comprises both protonation and reduction processes. From a thermodynamic point of view, there are three equivalent pathways for HAA, as depicted in the half-reaction thermodynamic cycle in Scheme 1. In total, five thermodynamic quantities are associated with this cycle. In addition to the (above-mentioned) $E°_H$, $E°$, and pK_a (further denoted as $pK_{a,ox}$), there is the one-electron reduction potential of the protonated form $Fe^{IV}OH$ ($E°'$) and the acidity constant of the reduced form $Fe^{III}OH$ ($pK_{a,red}$). The computed values of all of these quantities and their correlations are given in *SI Appendix*, Fig. S1 and Table S1. $E°_H$ is seen to correlate well with $E°$ (in particular for values of $E°$ greater than around −0.2 V). It is also noticeable that there is a very good correlation between $pK_{a,red}$ and $pK_{a,ox}$, as well as between $E°$ and $E°'$. Together, these findings indicate that the dominant contribution to a half-reaction thermodynamic driving force for HAA arises from the electrophilicity of the ferryl complex, but this trend becomes somewhat lost at low $E°$ values due to an increased role of basicity.

The computed data raise a fundamental question as to whether the redox and acidobasic properties of the ferryl complex correlate with the activation barrier in HAA, which is usually viewed as a concerted process with some degree of asynchronicity in H^+/e^- transfers. To address this issue, we introduce two thermodynamic descriptors, "effective electrophilicity" and "effective basicity", which we consider to reflect the coupled nature of both transfers, and thus, to be key factors driving an HAA process and significantly codetermining its character (e.g., asynchronicity of H^+/e^- transfers in HAA).

Considering the thermodynamic equivalence of the three pathways connecting $Fe^{IV}O$ with $Fe^{III}OH$ in Scheme 1, the following equation is easily derived:

$$E°_H = E°_{eff} + RT/F \times \ln(10) \times pK_{a,eff}, \quad [1]$$

where $E°_{eff}$ [$\equiv$½($E°$ + $E°'$)] is the effective reduction potential averaged over the nonprotonated and protonated forms; $pK_{a,eff}$ [$\equiv$½($pK_{a,red}$ + $pK_{a,ox}$)] corresponds to the effective acidity constant averaged over the reduced and oxidized forms; R is the universal gas constant (eV K^{-1}); T is temperature (K); F is the Faraday constant [F(e) = 1]; and $RT/F \times \ln(10)$ = 0.059 V at 298 K. $E°_{eff}$ can be interpreted as the potential for the attachment of an

electron to a "half-protonated" system, whereas $pK_{a,eff}$ can be viewed as an acidity constant associated with the abstraction of a proton from a "half-oxidized" complex. The proton-coupled reduction potential $E°_H$ is then directly linked to the free energy of the HAA reaction, ΔG_0, which can be obtained from the difference between $E°_H$ of a ferryl complex and that of the substrate ($\Delta E°_H$):

$$\Delta G_0[\mathrm{eV}] \equiv -F[\mathrm{e}] \times \Delta E°_H[\mathrm{V}] \equiv -F \times \left(E°_{\mathrm{H,FeO}} - E°_{\mathrm{H,sub}}\right). \quad [2]$$

Combining Eqs. **1** and **2**, ΔG_0 can be eventually expressed as a function of the two "effective" redox and acidobasic terms:

$$\Delta G_0 = -F \times \Delta E°_{\mathrm{eff}} - RT \times \ln(10) \times \Delta pK_{\mathrm{a,eff}}. \quad [3]$$

In Fig. 2*A*, an elegant and straightforward route to many important features associated with the effects of $\Delta E°_{\mathrm{eff}}$ vs. $\Delta pK_{\mathrm{a,eff}}$ on the HAA thermodynamic driving force (represented by $\Delta E°_H$) is outlined. First, the length and orientation of the $\Delta E°_H$ vector, which determines the magnitude and sign of the free energy of the HAT reaction (ΔG_0) according to Eq. **2**, is directly determined from a ($\Delta E°_{\mathrm{eff}}$, $0.059 \times \Delta pK_{\mathrm{a,eff}}$) point by its projection on the $\Delta E°_H$ diagonal axis, as indicated by dashed black lines. Note that any point lying on the diagonal that is perpendicular to the $\Delta E°_H$ axis and intersects the (0,0) origin (further referred to as a minor diagonal) describes an ergoneutral HAT reaction. Exergonic and endergonic reactions are associated with points located right and left from this minor diagonal, respectively. Second, the decomposition of $\Delta E°_H$ into redox vs. acidobasic ($\Delta E°_{\mathrm{eff}}$ vs. $0.059 \times \Delta pK_{\mathrm{a,eff}}$) components reveals which of the two factors makes a dominant favorable/unfavorable contribution to the HAA thermodynamic driving force. Third, the thermodynamic propensity for H^+/e^- transfer asynchronicity is elucidated by defining a parameter (η) as the dislocation of a point from the $\Delta E°_H$ axis, as depicted in Fig. 2*A*, obeying the equation:

$$\eta = 2^{-1/2} \times \left(\Delta E°_{\mathrm{eff}} - RT/F \times \ln(10) \times \Delta pK_{\mathrm{a,eff}}\right). \quad [4]$$

Note that the alternative expressions for the parameter η, which are derived from Eq. **4**, are given in *SI Appendix*. Thus, for $\eta \to 0$, the $\Delta E°_{\mathrm{eff}}$ and $\Delta pK_{\mathrm{a,eff}}$ components become comparably large, implying a more synchronous HAA process, which is demonstrated for various systems in the following section. For a point lying on the $\Delta E°_H$ axis, the redox and acidobasic contributions are equal; thus, any potential asynchronicity in the HAT mechanism cannot originate from these thermodynamic terms. Starting from the $\Delta E°_H$ diagonal and going in the downward direction, parallel to the minor diagonal, the propensity for a more asynchronous HAA process in favor of electron transfer (ET) is invoked (η gets more positive along this direction). Following the opposite direction, starting from the $\Delta E°_H$ diagonal, the propensity for a more asynchronous HAA process in favor of proton transfer (PT) is suggested (η gets more negative along this direction).

Fig. 2*B* shows key thermodynamic characteristics for two series of HAAs performed by the ferryl complexes in Fig. 1 [the series in blue is associated with HAA from cyclohexadiene (CHD), while the series in orange corresponds to HAA from phenol (PhOH)]. Among the HAA reactions with CHD (blue), the most exergonic one is associated with the most electrophilic/least basic complex, namely (CO)(TMC)Fe^{IV}O ($\Delta E°_H$ = +1.06 V; i.e., ΔG_0 = −24.4 kcal mol^{-1}), which is dominated by a strongly positive (favorable)

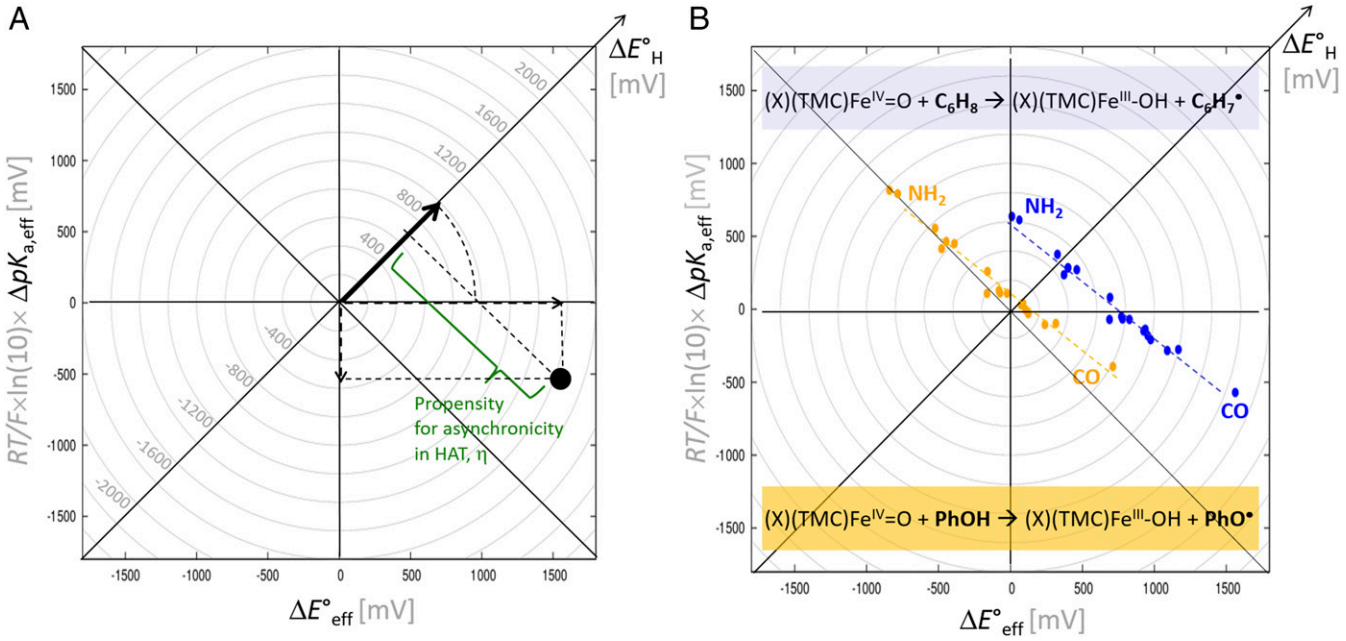

Fig. 2. (*A*) The correlation plot between $\Delta E°_{\mathrm{eff}}$ and $0.059 \times \Delta pK_{\mathrm{a,eff}}$ and their contributions to $\Delta E°_H$. The plot includes the following information: (*i*) the difference in proton-coupled reduction potentials between a ferryl complex and the substrate ($\Delta E°_H \equiv E°_{\mathrm{H,FeO}} - E°_{\mathrm{H,sub}}$), which is traced on the $\Delta E°_H$ diagonal and defines the endergonicity/exergonicity of the HAA reaction through the relationship $\Delta G_0 \equiv -F \times \Delta E°_H$ [the magnitude of a $\Delta E°_H$ vector is readily derived from the position of a ($\Delta E°_{\mathrm{eff}}$, $0.059 \times \Delta pK_{\mathrm{a,eff}}$) point as indicated by dashed lines]; (*ii*) the relative contributions of $\Delta E°_{\mathrm{eff}}$ ($\equiv E°_{\mathrm{eff,FeO}} - E°_{\mathrm{eff,sub}}$) and $\Delta pK_{\mathrm{a,eff}}$ ($\equiv pK_{\mathrm{a,eff,FeO}} - pK_{\mathrm{a,eff,sub}}$) to the HAT thermodynamic driving force ($\Delta E°_H$), being divided into octants that classify $\Delta E°_{\mathrm{eff}}$ vs. $\Delta pK_{\mathrm{a,eff}}$ contributions according to their favorable or unfavorable effect on $\Delta E°_H$ and their mutual dominance; (*iii*) the propensity for asynchronicity in the HAT reaction (η) quantified as the shortest distance of a ($\Delta E°_{\mathrm{eff}}$, $0.059 \times \Delta pK_{\mathrm{a,eff}}$) point from the $\Delta E°_H$ diagonal. The factor η is correlated with HAA reactivity and TS properties (Figs. 4 and 5). (*B*) $\Delta E°_{\mathrm{eff}}$ vs. $0.059 \times \Delta pK_{\mathrm{a,eff}}$ contributions to the HAA reactions between a ferryl complex from the TMC series in Fig. 1 and CHD and PhOH as substrates (blue and orange filled circles, respectively). The $E°_{\mathrm{eff}}$ and $0.059 \times pK_{\mathrm{a,eff}}$ values for the CHD and PhOH substrates are calculated to be −0.15 and 0.89 V (CHD) and 0.62 and 0.70 V (PhOH), and are shown along with $E°_{\mathrm{eff}}$ and $0.059 \times pK_{\mathrm{a,eff}}$ values for the (X)(TMC)Fe^{IV}O complexes in *SI Appendix*, Fig. S2.

redox term $\Delta E°_{eff}$ = +1.43 V, corresponding to $\Delta G_{E°eff}$ = −33.0 kcal mol^{-1}. Meanwhile, the acidobasic term 0.059 × $\Delta pK_{a,eff}$ makes a significant negative (unfavorable) contribution to the HAA thermodynamic driving force (−0.37 V, corresponding to $\Delta G_{pKa,eff}$ = +8.6 kcal mol^{-1}). The largest positive η value for this exergonic reaction (+1.28 V) suggests the highest propensity for asynchronicity in favor of ET (see the following section for more details). On the other hand, for the HAA reactions with the least electrophilic/most basic (X)(TMC)Fe^{IV}O complexes, ΔG_0 tends to result from more equal (and favorable) redox and acidobasic contributions. Specifically, for one of the strongest bases, namely (OH)(TMC)Fe^{IV}O, the $\Delta E°_{eff}$ and 0.059 × $\Delta pK_{a,eff}$ terms were calculated as +0.28 and +0.49 V, respectively. Due to the low η value, this base is predicted to abstract an electron and a proton in a more synchronous fashion. The only reactions with CHD that would tend to be significantly asynchronous in favor of PT involve the ferryl oxidant with either NH_2^- or enolate axial ligand (represented by the blue points lying near the vertical axis in Fig. 2*B*). Importantly, it appears that for some ferryl complexes, HAA reactions are equally exergonic, even though they differ significantly in η. This is exemplified for HAA reactions involving the ferryl complexes with NCS^- and OH^- axial ligands (both with ΔG_0 = −16.8 kcal mol^{-1}). For their reactions with CHD, the asynchronicity factors are η = +0.54 and −0.15 V, respectively.

Going from CHD to PhOH as the substrate, it can be seen in Fig. 2*B* that the series of points in orange (reactions with PhOH) shifts en masse left and upward with respect to the series of points in blue (reactions with CHD). This results in almost-ergoneutral reactions with PhOH. Near-ergoneutrality typically stems from a large compensation of two counteracting redox and acidobasic ($\Delta E°_{eff}$ and $\Delta pK_{a,eff}$) contributions to $\Delta E°_H$. The upward shift also means that many of the ferryl complexes predicted to abstract a hydrogen atom from the substrate CHD in favor of ET become potent for HAA processes that would proceed in a more synchronous manner, or in an asynchronous manner in favor of PT (this is in line with the more acidic character of the hydrogen atom in the substrate PhOH). For example, reactions of the substrate PhOH with ferryl complexes bearing NCS^- and OH^- as axial ligands are characterized by

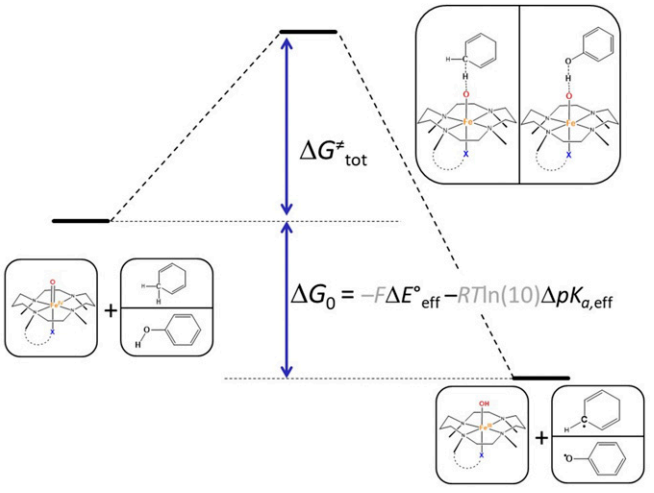

Scheme 2. Free-energy profile for HAA reaction between a ferryl complex (from Fig. 1) and the substrate CHD or PhOH. Free energies of activation and reaction ($\Delta G^{\neq}_{tot}$ and ΔG_0) are evaluated considering two noninteracting (separated) reactants and two separated products. We note that $\Delta G^{\neq}_{tot}$ is calculated as the free-energy difference between an S = 2 TS structure and the separated reactants in their lowest ground spin state (S = 1 or S = 2) and their lowest crossed or parallel conformation.

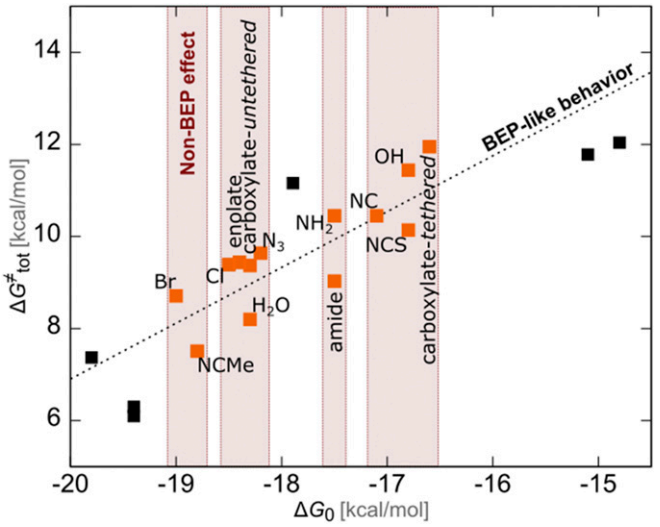

Fig. 3. A plot of $\Delta G^{\neq}_{tot}$ vs. ΔG_0 for HAA reactions of various (X)(TMC)Fe^{IV}O oxidants with CHD as the substrate. In general, the plot follows a BEP-like trend (dotted line). Significant deviation from this trend is found within four different highlighted regions that include points (in orange) differing in $\Delta G^{\neq}_{tot}$ for comparably large ΔG_0. The quantities $\Delta G^{\neq}_{tot}$ and ΔG_0 are defined in Scheme 2.

asynchronicity factors of η = −0.14 and −0.83 V, respectively, in contrast to the values of η = +0.54 (NCS^-) and −0.15 V (OH^-) for the analogous reactions with CHD. These observations may lead to mechanistic implications relevant for enzymatic selectivity: Depending on the native substrate to be activated (through homolytic cleavage of C–H, O–H, or N–H bonds), the effective redox vs. acidobasic properties of a metalloenzymatic catalytic site can be adjusted such that HAT proceeds more synchronously (or possibly more asynchronously in favor of PT) to avoid ET-controlled oxidations that may potentially be harmful to the fragile protein structure (27). These properties can be tuned without a significant effect on the overall HAT thermodynamic driving force.

To conclude, we suggest decomposition of the HAT thermodynamic driving force into redox and acidobasic components ($\Delta E°_{eff}$ and $\Delta pK_{a,eff}$) to define a thermodynamic propensity for asynchronicity in H^+/e^- transfers (represented by the parameter η), which we predict has an impact on the mechanism of the reaction and its energetics along the reaction coordinate. This has been investigated for a homologous series of ferryl complexes differing in an axial ligand and that computationally exhibit broad ranges of reduction potentials and of acidity constants. In the following section, we correlate the thermodynamic properties from Fig. 2*B* with some important reactivity features, such as activation free energies and transition-state (TS) electronic/geometric structure properties.

Effect of Redox Versus Acidobasic Thermodynamic Driving/Retarding Forces on the Free Energy of Activation and the Mechanism of HAT Reactions. The rate of an elementary reaction depends on the height of the free-energy barrier ($\Delta G^{\neq}_{tot}$ from Scheme 2), a tunneling factor, and a spin-transition probability if the ground spin state of the system is changed along the reaction trajectory. Here, we take advantage of the large variability in redox and acidobasic properties of these complexes to investigate the dependence of $\Delta G^{\neq}_{tot}$ on purely thermodynamic terms, namely ΔG_0 and the differential redox and acidobasic contributions to HAA, quantified by the asynchronicity factor η defined in the previous section.

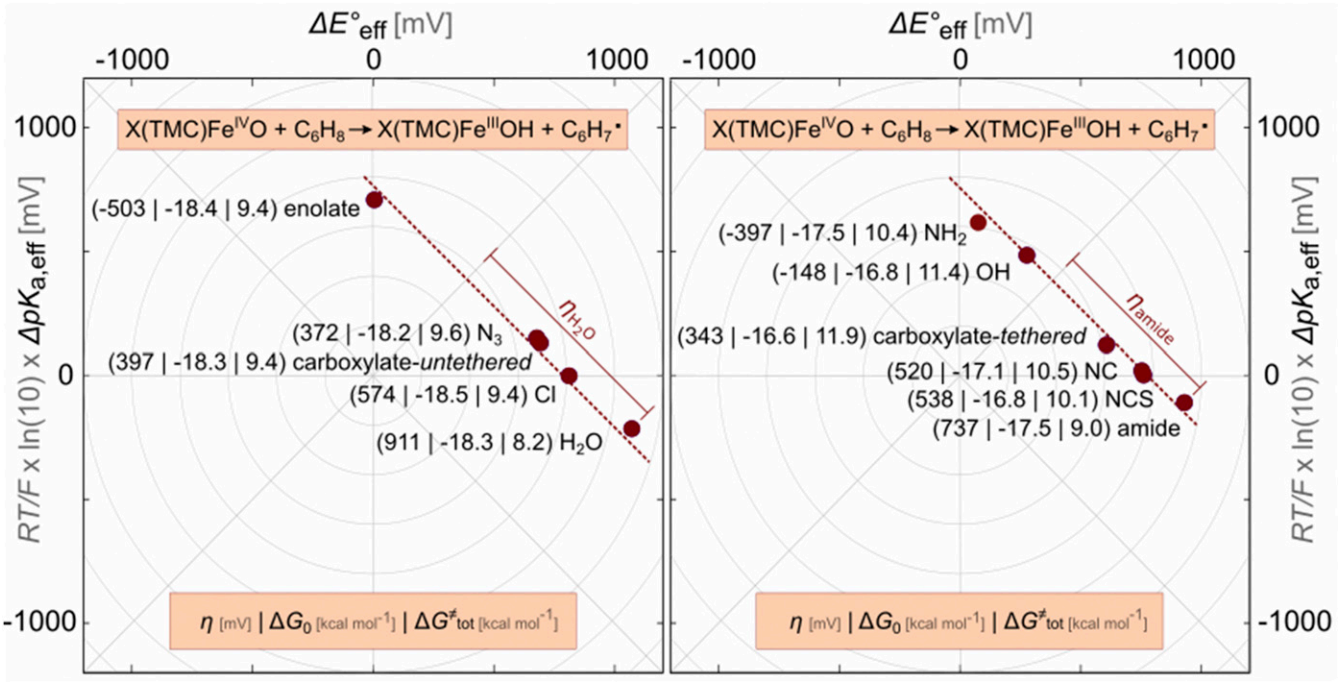

Fig. 4. For two different groups of points from Fig. 3, which do not follow the BEP-like trend and for which ΔG_0 is essentially the same, the reaction barrier $\Delta G^{\neq}_{tot}$ is correlated with the asynchronicity factor η derived from the square thermodynamic $RT/F \times \ln(10) \times \Delta pK_{a,eff}$ vs. $\Delta E°_{eff}$ plot.

First, from the $\Delta G^{\neq}_{tot}$ vs. ΔG_0 plot in Fig. 3, we note a general trend that a less exergonic reaction has to overcome a higher free-energy barrier. Such a relationship has been reported for many other systems (28–31) and is usually referred to as a BEP-like trend (BEP principle; originally formulated for enthalpies) (16, 17). However, a more detailed inspection of the $\Delta G^{\neq}_{tot}$ vs. ΔG_0 plot reveals patterns that cannot be rationalized on the basis of the BEP principle.

In Fig. 3, the non-BEP behavior is highlighted for HAA reactions with similar ΔG_0 but different $\Delta G^{\neq}_{tot}$. For example, this is the case for a pair of HAA reactions of CHD with the (NCS)(TMC)$Fe^{IV}O$ and (OH)(TMC)$Fe^{IV}O$ complexes, as discussed above. Although both reactions are equally exergonic (with $\Delta G_0 = -16.8$ kcal mol^{-1}), their $\Delta G^{\neq}_{tot}$ values differ by 1.3 kcal mol^{-1} in favor of (NCS)(TMC)$Fe^{IV}O$ (this and other examples are shown in Fig. 4). Although the two different trends indicated in Fig. 4 do not behave according to the BEP-like principle, we can clearly see a correlation of $\Delta G^{\neq}_{tot}$ with the factor η that reflects the propensity for asynchronicity in H^+/e^- transfers. Specifically, for reactions with CHD, a larger |η| gives rise to a lower activation free energy. This correlation between η and $\Delta G^{\neq}_{tot}$ suggests that ET/PT asynchronicity must translate into a characteristic feature of the TS. Indeed, for systems with a more positive η, we calculate TSs to be earlier in terms of C–H bond length and later in terms of the electron density transferred from CHD to the FeO complex. This is exemplified for some TS structures in Fig. 5.

To further elaborate on the dependence of $\Delta G^{\neq}_{tot}$ on η, we now focus on the reactivities of ferryl complexes with NCS^- vs. OH^- as axial ligands, with respect to the O–H bond of the PhOH substrate. In contrast to the analogous reactions with CHD, the $\Delta G^{\neq}_{tot}$ value for NCS is roughly 2.8 kcal mol^{-1} higher than that for OH. Changing the substrate, the relative effect of ΔG_0 on $\Delta G^{\neq}_{tot}$ remains the same for NCS vs. OH (i.e., there are no BEP-like contributions). Thus, the change of $\Delta\Delta G^{\neq}_{tot}$ (= $\Delta G^{\neq}_{tot}$[NCS] − $\Delta G^{\neq}_{tot}$[OH]) from −1.3 to +2.8 kcal mol^{-1} upon going from CHD to PhOH must be linked to another effect.

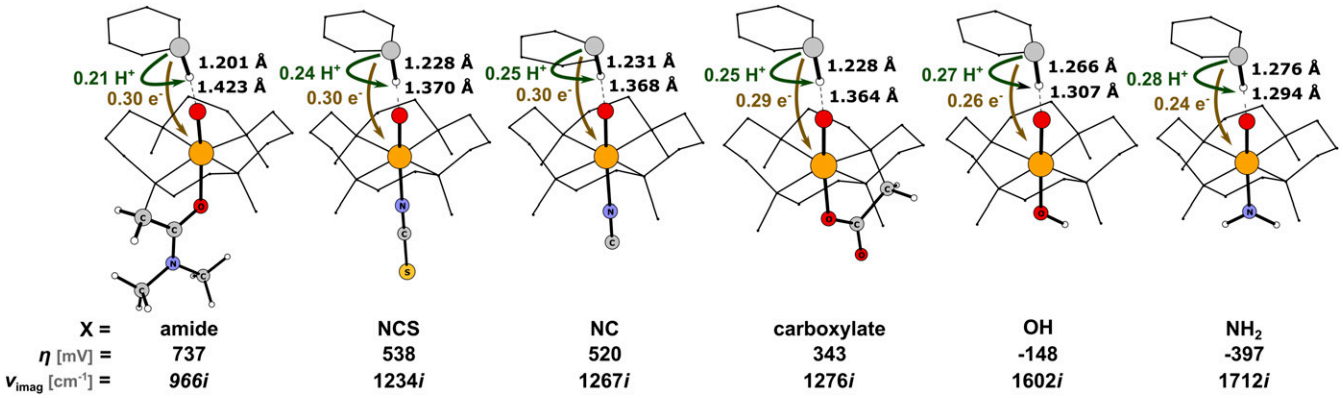

Fig. 5. TS geometries associated with reactions characterized in the *Right*-hand plot of Fig. 4, for which ΔG_0 is the same but η is different. For the series of six TSs, key geometric and electronic structure properties (as well as the imaginary frequencies of the TS reactive modes, ν_{imag}) are correlated with η.

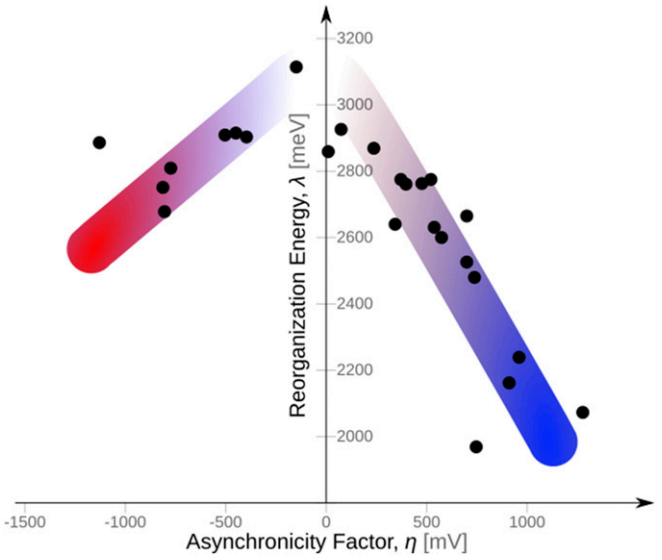

Fig. 6. Dependence of reorganization energy λ on asynchronicity factor η plotted for a series of 19 HAA reactions with the substrate CHD, specified in the previous section. The reorganization energy λ is derived from Eq. **6**. In addition to 19 HAA reactions with CHD, six others with three alternative substrates (*SI Appendix*, Table S2) are included to extend the λ vs. η plot into a negative region of the asynchronicity factor.

This effect can again be attributed to the asynchronicity factor η. In contrast to the situation for the HAA reactions with CHD, the NCS system is now associated with a smaller (less negative) η compared with OH (−0.14 vs. −0.83 V), which correlates with a higher $\Delta G^{\neq}_{tot}$. This is in line with our previous observation that a more synchronous reaction is associated with a higher $\Delta G^{\neq}_{tot}$.

It is also noteworthy that the magnitude of the imaginary frequency of the TS reactive mode $|\nu_{imag}|$ is dependent on η (Fig. 5). For a lower factor η, a larger value of $|\nu_{imag}|$ is calculated. The quantity $|\nu_{imag}|$ is a (mass-weighted) measure of the curvature of the barrier at the TS along the reaction coordinate. Thus, a larger $|\nu_{imag}|$ results from a sharper energy profile in the vicinity of the TS. This indicates a barrier with a smaller width, implying that tunneling (τ) plays a more important role in HAA reactivity (as a tunneling correction, $-RT \ln \tau$, to $\Delta G^{\neq}_{tot}$). Taking this into account, it appears that within the present set of HAA reactions with CHD, the most synchronous ones (i.e., with $\eta \rightarrow 0$) experience the largest tunneling contributions, which, to some extent, compensate for their highest $\Delta G^{\neq}_{tot}$. Following the findings indicating that a degree of tunneling is coupled to the asynchronicity factor, we predict that KIE increases as the asynchronicity factor η lowers. To unambiguously observe this correlation, it is necessary to eliminate a change in KIE due to effects derived from the BEP principle, and we propose model reactions from Fig. 5, which have essentially the same ΔG_0, as candidates to test this observation.

It is important to note that spin-transition probability of some (X)(TMC)$Fe^{IV}O$ complexes has been suggested to be rate determining for HAA reactions (12, 25). While this effect might contribute to C–H activation by metal–oxo complexes, we consider that the thermodynamic bias, as introduced in the factor η, is a straightforward step toward a more general and unified description of the HAA process.

Thus, it has been clearly shown that together with ΔG_0, the asynchronicity parameter η, determined from pure thermodynamic properties of both the substrate and oxidant (Fig. 2), is an important factor that contributes to the height and width of the reaction barrier. This factor may also contribute to deviations from the classical BEP-like dependence of $\Delta G^{\neq}_{tot}$ on ΔG_0.

Coupled Proton and Electron Transfers: Asynchronicity and Its Connection to Reorganization Energy in Marcus Theory. According to the Marcus theory for bimolecular ET reaction, the total activation free energy is given as a function of three thermodynamic terms: the free energy of formation of the reactant complex (w_R); the free energy of reaction ($\Delta G_{0,R}$), which is defined as the free-energy difference between the product and reactant complexes; and the reorganization energy (λ), which is the energy required for a perturbation of the system structure to proceed from reactant to product complex coordinates, without any ET:

$$\Delta G^{\neq}_{tot} = w_R + \frac{\lambda}{4}\left(1 + \frac{\Delta G_{0,R}}{\lambda}\right)^2. \quad [5]$$

Note that $\Delta G_{0,R}$ in Eq. **5** is equal to $\Delta G_0 + w_P - w_R$ as derived from Scheme S1, where w_R and w_P represent the free energy of formation of the reactant and product complexes, respectively (ΔG_0 is defined in Scheme 2). Assuming that $\lambda >> |\Delta G_0 + w_P - w_R|$, then Eq. **5** also applies to HAT (5). As a result, after expansion and truncation of the quadratic term in Eq. **5** and considering $w_P = w_R$ (for a detailed derivation, see *SI Appendix*), we can approximate λ for a bimolecular HAA reaction as:

$$\lambda/4 = \Delta G^{\neq}_{tot} - w_R - \Delta G_0/2, \quad [6]$$

where w_R is defined as earlier and $\Delta G^{\neq}_{tot}$ and ΔG_0 are calculated according to Scheme 2 (for ΔG_0, see also Eq. **2**). Calculation of λ

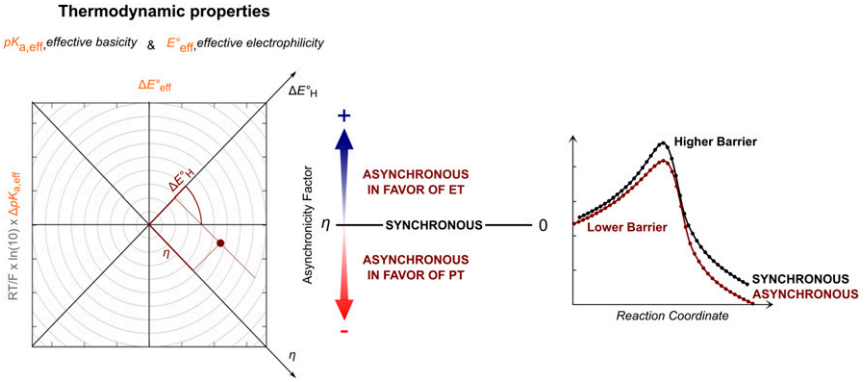

Scheme 3. Differences in effective redox and acidobasic quantities between the oxidant and the substrate determine the factor η (*Left*) that quantifies a propensity for asynchronicity in H^+/e^- transfers in concerted HAA reactions (*Middle*); η further correlates with the height and width of the reaction barrier (*Right*).

from Eq. **6** and its correlation with the calculated asynchronicity factor η (defined by Eq. **4** as derived from Fig. 2*A*) leads to the most stunning finding reported in this work, presented in Fig. 6.

According to Fig. 6, HAA reactions that are predicted as the most asynchronous in favor of ET (i.e., with the most positive η) are also associated with the lowest λ. On moving toward more synchronous reactions, λ increases, reaching its maximum when η approaches 0, and then it decreases once more on moving further toward more asynchronous reactions in favor of PT. In addition to the "volcano" character of the λ vs. η correlation in Fig. 6, we note that a change in η almost quantitatively induces an opposite change in λ. Such a correlation arises mainly for two reasons. First, we are considering a set of homologous reactions, which allows the elimination of additional (i.e., steric and electronic) contributions to $\Delta\Delta G^{\neq}_{tot}$ that would otherwise arise from different interactions of the substrate with the $Fe^{IV}O$ oxidant at the TSs. Second, these homologous reactions are comparably adiabatic, as reflected by an electronic coupling between the "reactant" and "product" states at the TSs that is approximately constant for all reactions in the series (*SI Appendix*, Fig. S3; for more details on electronic coupling and its effect on the barrier see *SI Appendix*). Thus, keeping these steric effects as well as (non)adiabaticity constant across the series, the plot in Fig. 6 demonstrates the intimate relationship between the thermodynamic quantity η and the reorganization energy.

From this perspective, we conclude that for a set of homologous reactions, the disparity between effective redox and acidobasic (ΔE°_{eff} and $\Delta pK_{a,eff}$) contributions to the HAT thermodynamic driving force (ΔE°_{H}) is exclusively responsible for the variations in reorganization energy, which is one of few factors (ΔG_0 and λ) contributing to the Marcus free-energy barrier. This could provide a powerful guideline for a tailored design of new HAT catalysts of preferred reactivity and selectivity by tuning the experimentally attainable and chemically more intuitive asynchronicity factor (note that the limitations of the concept are briefly discussed in *SI Appendix*).

To view the concept of asynchronicity factor (as implemented into Marcus theory) in the context of other models, Warren and Mayer's (15) application of the Marcus cross-relation to a broad spectrum of HAA reactions is noticeable. Within this model, reorganization energy λ for HAT from HA to B is approximated as the mean of two intrinsic λ's for two self-exchange HA/A and HB/B reactions (referred to as additivity postulate). As pointed out by Warren and Mayer (15), the attractiveness of this treatment is given by its simplicity and good predictive power despite its reliance on the crude additivity postulate that ignores a dependence of a reagent on its partner. However, the additivity postulate appears to fail, for example, in the case of HAA reactions with significant polar (PME-like) effects in the TS. In this respect, we predict our methodology to provide a more general and chemically more intuitive explanation for trends in λ (and thus in $\Delta G^{\neq}$) for HAA reactions, including those with significant PME-like effects in the TS, which are inherent to the model of asynchronicity factor as documented in Fig. 5.

Conclusions

Depending on the electron-donating ability of the ligand in the $Fe^{IV}O$ complex, the associated reduction potentials (E°) and acidity constants ($pK_{a,ox}$) were calculated to vary over ranges of around 1.2 V and 20 pK_a units, respectively. Such large changes in both properties across the series provided a good basis for the study of redox vs. acidobasic effects on the HAA free-energy barriers associated with these compounds. The HAA reaction is intrinsically a coupled transfer of one proton and one electron from a substrate to an oxidant. In this context, we first defined two thermodynamic driving quantities that both inherently reflect the coupled nature of H^+ and e^- transfers involved in HAA; namely, the effective reduction potential (E°_{eff}) and the effective acidity constant ($pK_{a,eff}$). The former corresponds to the reduction potential averaged over the $Fe^{IV}O$ and $Fe^{IV}OH$ complexes, while the latter is defined as the average acidity constant associated with the $Fe^{IV}OH$ and $Fe^{III}OH$ species.

Having evaluated these quantities for the oxidant and the substrate, the HAA thermodynamic driving force corresponding to the difference in proton-coupled reduction potential between the oxidant and the substrate (ΔE°_{H}) can be decomposed into effective redox (ΔE°_{eff}) and acidobasic ($\Delta pK_{a,eff}$) contributions, as illustrated in Scheme 3, *Left*. This decomposition allows us to define the asynchronicity factor η, which is a measure of the propensity for asynchronicity in concerted H^+/e^- transfers due to a disparity between ΔE°_{eff} and $\Delta pK_{a,eff}$ contributions to the HAA thermodynamic driving force (Scheme 3, *Left* and *Middle*). Evaluation of HAA energetics for nineteen reactions revealed an important effect of η on the calculated barrier. Thus, η is a thermodynamic factor, in addition to the free energy of reaction (ΔG_0), which has the potential to modulate the height and width of the barrier (Scheme 3, *Right*). In the context of Marcus theory, the asynchronicity factor η was further correlated with the reorganization energy λ, evidencing that a change in η almost quantitatively corresponds to an opposite change in λ such that a synchronous HAT reaction (having η equal to 0) has the highest λ. For reactions with the same ΔG_0, those classified as being more synchronous are thus associated with a higher reaction barrier.

In summary, we have described the dependence of an HAA barrier on the asynchronicity factor, which we further consider to be of general importance in HAA catalysis. We suggest an appealing possibility of using this thermodynamic parameter for tuning HAA reactivity and selectivity toward various substrate C–H, O–H, or N–H bonds. Variation of effective redox vs. acidobasic contributions through the modification of an axial ligand in the coordination sphere of a catalytic site (as demonstrated here for a large set of nonheme ferryl complexes) serves as an example of such a strategy. The validity of our model that accounts for asynchronicity contributions to free-energy activation barriers can be examined in different areas of HAA chemistry, whenever the BEP-like principle is not followed and/or whenever a rather qualitative PME concept has been invoked. The factor of asynchronicity may quantitatively rationalize experimental observations such as, for example, selective activation of stronger aliphatic C–H bonds in the presence of weaker ones (18, 32, 33) or rate-enhancing/retarding effects of the solvent on HAA reactions with essentially no change in their reaction equilibrium constants (34).

Methods

Computational details are provided in *SI Appendix*.

ACKNOWLEDGMENTS. We thank Czech Science Foundation Grants 15-10279Y and 18-13093S; Czech Academy of Sciences Grant RVO 61388963 for financial support; and the Ministry of Education, Youth and Sports (LM2015070, Large Infrastructures for Research, Experimental Development and Innovations: IT4Innovations National Supercomputing Center) for computing time.

1. Warren JJ, Tronic TA, Mayer JM (2010) Thermochemistry of proton-coupled electron transfer reagents and its implications. *Chem Rev* 110:6961–7001.
2. Huynh MHV, Meyer TJ (2007) Proton-coupled electron transfer. *Chem Rev* 107: 5004–5064.
3. Rokob TA, et al. (2016) Mono- and binuclear non-heme iron chemistry from a theoretical perspective. *J Biol Inorg Chem* 21:619–644.
4. Krebs C, Galonić Fujimori D, Walsh CT, Bollinger JM, Jr (2007) Non-heme Fe(IV)-oxo intermediates. *Acc Chem Res* 40:484–492.

5. Migliore A, Polizzi NF, Therien MJ, Beratan DN (2014) Biochemistry and theory of proton-coupled electron transfer. *Chem Rev* 114:3381–3465.
6. Mayer JM, Hrovat DA, Thomas JL, Borden WT (2002) Proton-coupled electron transfer versus hydrogen atom transfer in benzyl/toluene, methoxyl/methanol, and phenoxyl/phenol self-exchange reactions. *J Am Chem Soc* 124:11142–11147.
7. Sirjoosingh A, Hammes-Schiffer S (2011) Proton-coupled electron transfer versus hydrogen atom transfer: Generation of charge-localized diabatic states. *J Phys Chem A* 115:2367–2377.
8. Hammes-Schiffer S, Stuchebrukhov AA (2010) Theory of coupled electron and proton transfer reactions. *Chem Rev* 110:6939–6960.
9. Mayer JM (2011) A simple Marcus-theory type model for hydrogen atom transfer/proton-coupled electron transfer. *J Phys Chem Lett* 2:1481–1489.
10. Tishchenko O, Truhlar DG, Ceulemans A, Nguyen MT (2008) A unified perspective on the hydrogen atom transfer and proton-coupled electron transfer mechanisms in terms of topographic features of the ground and excited potential energy surfaces as exemplified by the reaction between phenol and radicals. *J Am Chem Soc* 130: 7000–7010.
11. Mandal D, et al. (2015) How does tunneling contribute to counterintuitive H-abstraction reactivity of nonheme Fe(IV)O oxidants with alkanes? *J Am Chem Soc* 137:722–733.
12. Kwon YH, et al. (2015) Determination of spin inversion probability, H-tunneling correction, and regioselectivity in the two-state reactivity of nonheme iron(IV)-oxo complexes. *J Phys Chem Lett* 6:1472–1476.
13. Mandal D, Mallick D, Shaik S (2018) Kinetic isotope effect determination probes the spin of the transition state, its stereochemistry, and its ligand sphere in hydrogen abstraction reactions of oxoiron(IV) complexes. *Acc Chem Res* 51:107–117.
14. Minakata D, Crittenden J (2011) Linear free energy relationships between aqueous phase hydroxyl radical reaction rate constants and free energy of activation. *Environ Sci Technol* 45:3479–3486.
15. Warren JJ, Mayer JM (2012) Application of the Marcus cross relation to hydrogen atom transfer/proton-coupled electron transfer reactions. *Proton Coupled Electron Transfer: A Carrefour of Chemical Reactivity Traditions*, eds Formosinho S, Barroso M (Royal Soc Chem, Cambridge, UK), pp 1–31.
16. Bell RP (1936) The theory of reactions involving proton transfers. *Proc R Soc Lond A* 154:414–429.
17. Evans MG, Polanyi M (1938) Inertia and driving force of chemical reactions. *Trans Faraday Soc* 34:11–24.
18. Le C, Liang Y, Evans RW, Li X, MacMillan DWC (2017) Selective sp^3 C-H alkylation via polarity-match-based cross-coupling. *Nature* 547:79–83.
19. Tedder JM (1982) Which factors determine the reactivity and regioselectivity of free radical substitution and addition reactions? *Angew Chem Int Ed Engl* 21:401–410.
20. Paul V, Roberts BP (1987) Polarity reversal catalysis of hydrogen atom abstraction reactions. *J Chem Soc Chem Commun* 17:1322–1324.
21. Roberts BP (1998) Polarity-reversal catalysis of hydrogen-atom abstraction reactions: Concepts and applications in organic chemistry. *Chem Soc Rev* 28:25–35.
22. Puri M, Que L, Jr (2015) Toward the synthesis of more reactive S = 2 non-heme oxoiron(IV) complexes. *Acc Chem Res* 48:2443–2452.
23. Sastri CV, et al. (2007) Axial ligand tuning of a nonheme iron(IV)-oxo unit for hydrogen atom abstraction. *Proc Natl Acad Sci USA* 104:19181–19186.
24. England J, et al. (2014) An ultra-stable oxoiron(IV) complex and its blue conjugate base. *Chem Sci (Camb)* 5:1204–1215.
25. Bigelow JO, et al. (2017) Oxoiron(IV) tetramethylcyclam complexes with axial carboxylate ligands: Effect of tethering the carboxylate on reactivity. *Inorg Chem* 56: 3287–3301.
26. Bím D, Rulíšek L, Srnec M (2018) Computational electrochemistry as a reliable probe of experimentally elusive mononuclear non-heme iron species. *J Phys Chem C* 122:10773–10782.
27. Yosca TH, et al. (2013) Iron(IV)hydroxide pK(a) and the role of thiolate ligation in C-H bond activation by cytochrome P450. *Science* 342:825–829.
28. Mayer JM (2011) Understanding hydrogen atom transfer: From bond strengths to Marcus theory. *Acc Chem Res* 44:36–46.
29. Kwon E, Cho K-B, Hong S, Nam W (2014) Mechanistic insight into the hydroxylation of alkanes by a nonheme iron(V)-oxo complex. *Chem Commun (Camb)* 50:5572–5575.
30. Ghosh M, et al. (2014) Formation of a room temperature stable Fe(V)(O) complex: Reactivity toward unactivated C-H bonds. *J Am Chem Soc* 136:9524–9527.
31. Xue X-S, Ji P, Zhou B, Cheng J-P (2017) The essential role of bond energetics in C-H activation/functionalization. *Chem Rev* 117:8622–8648.
32. Barham JP, John MP, Murphy JA (2016) Contra-thermodynamic hydrogen atom abstraction in the selective C-H functionalization of trialkylamine N-CH_3 groups. *J Am Chem Soc* 138:15482–15487.
33. O'Reilly RJ, et al. (2011) Hydrogen abstraction by chlorine atom from amino acids: Remarkable influence of polar effects on regioselectivity. *J Am Chem Soc* 133: 16553–16559.
34. Warren JJ, Mayer JM (2010) Predicting organic hydrogen atom transfer rate constants using the Marcus cross relation. *Proc Natl Acad Sci USA* 107:5282–5287.